Supporting Information

Saturation of LacI with model constructs

Complete binding of LacI to the model constructs was ensured by titrating concentrated LacI solution into a solution containing hybridized model constructs until saturation in the FPA value was observed. A typical titration curve is shown in Figure S1. Experiments with LacI were carried out with a constant Na^+ concentration of 300 mM.

To ensure that LacI was not bound non-specifically to parts of the model construct other than the operon sequence under our experimental conditions of 50 mM MOPS, pH 7.0 and 280 mM NaCl, we designed a non-specific binding model construct (NS-MC) that does not have the operon sequence and can only bind LacI nonspecifically. NS-MC is a DNA analog of MC-3A (Table 1B) with the operon sequence of MC-3A replaced with 5'-TGC AAT GGT GCA CCA TTG CA-3'. Titration of concentrated LacI solution into hybridized NS-MC causes no change in observed anisotropy (Fig. S1), indicating that there is no nonspecific binding of LacI at 300 mM Na^+. Nonspecific binding of LacI is significant at lower counter-ion concentration ([1], data not shown) so these conditions were not used herein for experiments with LacI.

Thermal and motional properties of 6-MI in helices

6-MI is a guanosine analog that can be site specifically incorporated into DNA helices or hybrid DNA/RNA helices [2,3]. The base paring ability of 6-MI can be tested by thermal melting experiments. Replacing guanosine with 6-MI has virtually no effect on the thermal stability of DNA helixes ([3] and Table S1). In RNA duplexes, a 6-MI•C base pair is destabilizing compared to a G•C base pair but is stabilizing compared to an A•C

mismatch (Table S1). Further, KI quenching experiments showed that 6-MI in a RNA duplex is not solvent accessible (Fig. S2), implying that despite the lessened energetic contribution from base pairing 6-MI remains in a stacked conformation.

Fluorescence lifetime measurement and base sequence requirements for the 6-MI experiments

Fluorescence lifetimes of 6-MI free in solution and 6-MI in selected DNA and RNA duplexes were measured and summarized in Table S2. Samples (1 μM) were annealed in buffer A (50 mM MOPS, 20 mM NaCl, 10 mM $MgCl_2$, pH 7.0) and were placed in a temperature-controlled housing at 15℃. Repetitive pulsed laser excitation (Coherent Mira Titanium-Sapphire laser, frequency-tripled at 321 nm with pulse width ca. 1 ps) was applied and fluorescence emission was detected under magic angle conditions at 431 nm. A microchannel plate photomultiplier (Hamamatsu R3809U-01) and standard time-correlated, single-photon counting electronics were used for detection. Emission decays were recorded in 4096 channels with a time increment of 8.9 ps/channel until at least 50,000 counts were collected. The instrument response function was recorded using scattered light from a dilute suspension of nondairy coffee creamer. Emission decays were fit to a sum of exponential functions using custom software performing non-linear least squares fits following convolution of the fitting function with the instrument response function. The goodness of fit was determined by the value of χ^2 and by examination of the weighted residuals.

The sequences of our oligomers were designed to have two pyrimidines on each side of the 6-MI to minimize quenching and maintain longer fluorescence lifetime.

Hawkins et al. has observed that 6-MI is strongly quenched by immediately adjacent purines and to a lesser extent by purines in the second neighboring position [3]. Furthermore, our 6-MI containing RNA or DNA constructs were designed with only uracil or thymine, respectively, immediately adjacent to 6-MI to better shield 6-MI from guanine, which is generally the most efficient fluorescence quencher among the nucleic acid bases[4]. With this sequence, a mean lifetime of over 2 ns was observed for 6-MI in DNA duplexes and over 4 ns in RNA duplexes (Table S2). In contrast, the mean lifetime for 6-MI-containing duplexes [3] was only 0.53 ns with an immediately adjacent cytosine.

FPA of DNA duplexes of different length

Four DNA duplexes, 11mer, 23mer, 35mer and 47mer are used herein. Initial experiments were carried out without ligating the 6-MI-containing strand. "Nicked" 23mer and 47mer duplexes gave the same anisotropy as the corresponding ligated, continuous 23mer and 47mer, respectively (Table S3). We therefore used the nicked 35mer duplex in the experiments' of Figure 2 and treated this nicked duplex as if it were a continuous duplex of that length. The sequences of the four DNA duplexes are listed in Table 1C.

By modeling a DNA duplex as cylinder of finite length, the motion of DNA can be characterized by the rotational diffusion coefficient about the symmetry (long) axis of DNA, $D_{\|}$, and about the axis perpendicular to the long axis, $D_{\perp}$. Assuming that the absorption and emission dipoles of 6-MI are collinear and perpendicular to the long axis of the DNA duplex, the steady state anisotropy, r, of 6-MI labeled DNA duplexes can be approximated assuming a single exponential decay of 6-MI:

$$r = r_o\left(\frac{0.25}{1+\frac{\tau}{\tau_1}}+\frac{0.75}{1+\frac{\tau}{\tau_2}}\right) \qquad \text{(eq. S1)},$$

where $r_\circ = 0.345$ is the observed limiting anisotropy (the average of $r_\circ$ of the four DNA duplexes of different lengths, Table 1C) , τ is the mean lifetime of 6-MI and τ_1 and τ_2 are the rotational correlation time along the long axis and short axis of DNA.

$\tau_1 = (4D_{\|} + 2D_{\perp})^{-1}$ and $\tau_2 = (6D_{\perp})^{-1}$ 4. $D_{\|}$ and $D_{\perp}$ can be calculated based on the expressions derived by Tirado and Garcia de la Torre[5,6]:

$$D_{\perp} = \frac{3k_BT}{\pi\eta L^3}(\ln(p) + \delta_{\perp}) \text{ and } D_{\|} = \frac{k_BT}{3.814\pi\eta L^3}(\frac{4p^2}{1+\delta_{\|}}) \qquad \text{(eq. S2)},$$

where k_B is Boltzmann constant, L is the length of DNA, d is the hydrodynamic diameter of DNA, p = L/d, $\delta_{\|} = (1.119 \times 10^{-4} + 0.6884/p - 0.2019/p^2)$, and $\delta_{\perp} = (-0.662 + 0.917/p - 0.05/p^2)$. L is calculated assuming 0.34 nm rise per base pair, and d is assumed to equal to 2 nm. The experimental temperature of 15 °C gives a viscosity of $\eta = 1.14$ cp. From equation S1, the expected anisotropy is a function of the rotational correlation time along both the long (τ_1) and short (τ_2) axis of DNA duplex. The rotational motion along either direction causes the anisotropy to be smaller than the limiting anisotropy $r_\circ$. $r = r_\circ - r_1 - r_2$, where r_1 and r_2 are anisotropy contribution from τ_1 and τ_2, respectively. Figure S3 shows that both τ_1 and τ_2 increase with DNA length, and the resulting anisotropy approaches $r_\circ$. The impact of τ_1 is always larger than τ_2 and the impact of τ_1 diminishes less than τ_2 with increasing DNA length. For duplexes 35mer or longer, the impact from τ_2 is negligible relative to the experimental uncertainty.

Estimating the anisotropy of simple duplexes with LacI bound

Binding of LacI increases the overall size of the system and causes both τ_1 and τ_2 to increase, which results in anisotropy value closer to $r_\circ$. Consider a hypothetical situation where LacI is tightly bound to the 47mer DNA duplex in a 1:1 ratio. With a molecular weight of 154 kDa, the volume of LacI can be estimated to be about 180 nm^3 [7]. The molecular volume of the 47mer DNA can be approximated to be about 26.4 nm^3 assuming 0.281 nm^3 per nucleotide [8]. The overall volume of the DNA/protein complex is dominated by the protein. Since the DNA/protein complex has an irregular shape and predicting the rotational correlation time based on a complex shape is very difficult, we estimated the rotational correlation time of the complex using an empirical rule that the observed rotational correlation time of a protein is about twice of a corresponding sphere[4,9] : $\tau_1 = \tau_2 = 2*(\eta V)/kT$ = 118.6 ns, where η = 1.14 cp, V = 180.4+ 26.4 = 206.8 nm^3, k is the Boltzmann constant, T = 288.15 K. The anisotropy can be predicted the same way as for the DNA duplexes using equation S1. The calculated anisotropy for the DNA/protein complex is 0.339 compared to 0.308 for the DNA alone. The anisotropy of the DNA protein complex is within 0.006 of $r_\circ$, whereas that for the DNA duplex alone is ~0.04 lower than $r_\circ$. Thus, binding of LacI slows the overall motion of the complex and greatly reduces its contribution to the observed anisotropy. We assume that the small remaining motion is inconsequential.

Normalization of FPA of model constructs

The salt dependence of the FPA of the model constructs were normalized relative to the FPA of 11mer duplex to account for salt effects on the internal motion of the 6-MI

fluorophore (Figure S4). r_{norm} is calculated as the ratio between the apparent rotational correlation time, θ, of the constructs and the 11mer duplex only, $r_{norm} = \theta_{construct} / \theta_{11mer}$. θ is related to the rate of anisotropy decay, with larger θ associated with higher anisotropy. To simplify calculation, the basic Perrin equation for a sphere, $r = r_{\circ} \left(\frac{1}{1+\frac{\tau}{\theta}} \right)$, where τ is the lifetime of 6-MI (Table S2), was used to obtain r_{norm}. $r_{norm} = (\frac{r_{\circ}}{r_{11mer}} - 1) / (\frac{r_{\circ}}{r_{construct}} - 1)$, where $r_{\circ} = 0.33$ of the 11mer was used for all of the constructs.

Table S1. Comparison of melting temperatures of DNA and RNA duplexes with a G•C base pair, a F•C base pair or an A•C mismatch. As 6-MI is only available in the deoxynucleotide form, a dG•C version of the RNA duplex was also compared. The solution conditions were 50 mM MOPS, pH 7.0, 1 M NaCl with 1μM of each strands.

Duplex	**T_m (°C)**
DNA/DNA	
d(CCCTCTT**G**TCC)/d(GGA**C**AGGAGGG)	39.1 ± 0.7
d(CCCTCTT**F**TCC)/d(GGA**C**AGGAGGG)	40.2 ± 0.1
d(CCCTCTT**A**TCC)/d(GGA**C**AGGAGGG)	≤13
RNA/RNA	
r(CCCUCUU**G**UCC)/r(GGA**C**AGGAGGG)	67.9 ± 0.5
r(CCCUCUU**F**UCC)/r(GGA**C**AGGAGGG)	56.0 ± 0.2
r(CCCUCUU**dG**UCC)/r(GGA**C**AGGAGGG)	64.4 ± 0.7
r(CCCUCUU**A**UCC)/r(GGA**C**AGGAGGG)	50.4 ± 0.4

Table S2. Fluorescence lifetimes of free 6-MI in solution and 6-MI in DNA or RNA duplexes. Conditions: 50 mM sodiumMOPS, pH 7.0, 10 mM $MgCl_2$, 15 °C.

*The DNA duplex is the same as in Table S1. The RNA 11mer is the corresponding RNA version of the DNA 11mer.

†Mean life time $\bar{\tau} = \sum_i \alpha_i \tau_i$.

Sample*	Lifetime (ns)	Amplitudes	Mean lifetime (ns)
6MI	5.87 ± 0.05	1.00	5.87 ± 0.05
DNA (11 mer)	5.68 ± 0.16 2.21 ± 0.02 0.16 ± 0.01	0.12 ± 0.01 0.70 ± 0.01 0.18 ± 0.01	2.26 ± 0.12
RNA (11 mer)	5.44 ± 0.05 2.26 ± 0.23 0.10 ± 0.01	0.75 ± 0.03 0.13 ± 0.01 0.12 ± 0.02	4.39 ± 0.24

Table S3. Comparison of anisotropy of continuous and nicked DNA duplexes. Conditions: 50 mM sodiumMOPS, pH 7.0, 10 mM Mg^{2+}, 15 °C. The sequence of the continuous 23mer and 47mer is in Table S1. The nick site is shown in Table S1 for the 35mer.

	continuous	nicked
23 mer	0.271 ± 0.003	0.274 ± 0.003
47mer	0.281 ± 0.003	0.285 ± 0.003

Figure legends

Figure S1. Titration of MC-3A (●, ▲) and the non-specific binding model construct (NS-MC) (○) with increasing LacI. Conditions: 50 mM sodiumMOPS, pH 7.0, 280 mM NaCl, 15 °C with 0.25 (●) or 1.25 (▲,○) μM of model constructs with 100 nM of 6-MI containing short strands.

Figure S2. Effect of the collisional quencher KI on the fluorescence emission of 6-MI incorporated into single-stranded and double-stranded DNA and RNA oligonucleotides. Buffer conditions: 50 mM MOPS, pH 7.0, 10 mM $MgCl_2$ and 15 °C. F_o is the fluorescence intensity in the absence of KI. The 6-MI-containing single-stranded RNA is S_{Fc} (Table S1), ○, and the single-stranded DNA is the DNA version of

S_{Fc}, □. The double-stranded RNA, ●, and DNA, ■, include a non-fluorescence complementary strand.

Figure S3. Estimated rotational correlation time along the long and short axis of DNA duplexes. (See Supporting information text).

Figure S4. The Mg^{2+} dependence of anisotropy (top) and the normalized anisotropy (r_{norm}) (See Supporting information text) (bottom) of model constructs with LacI bound: model constructs 3A (●); 3U (○); PEG (▲) and 11 mer control (▼). Conditions: 50 mM NaMOPS, pH 7.0, 280 mM NaCl, 15 °C. The oligonucleotide used is S_F.

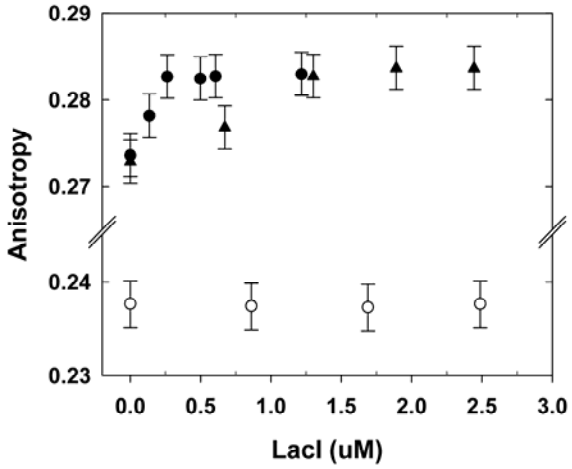

Figure S1

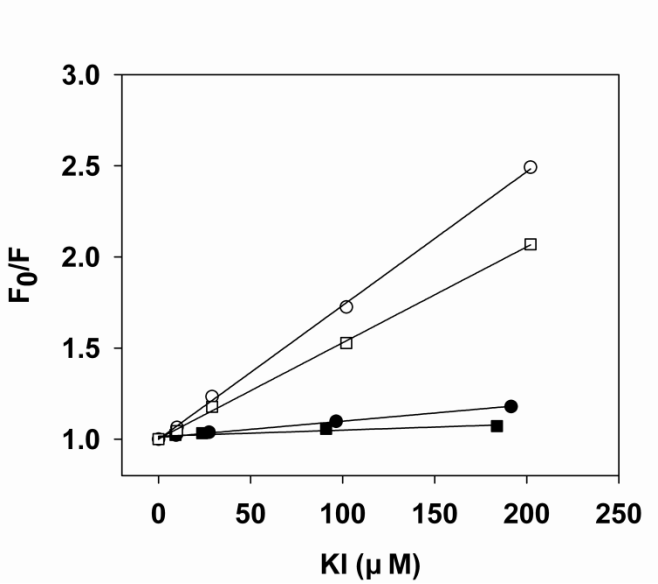

Figure S2

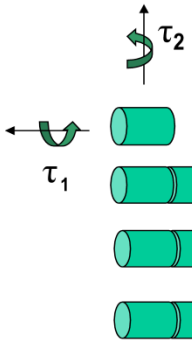

	τ_1 (ns)	τ_2 (ns)	r_1	r_2	r
11 mer	3.4	6.0	0.103	0.024	0.218
23 mer	7.1	25.6	0.063	0.007	0.275
35 mer	10.7	66.1	0.045	0.003	0.297
47 mer	14.3	133.0	0.035	0.001	0.308

$r = r_0 - r_1 - r_2$

Figure S3

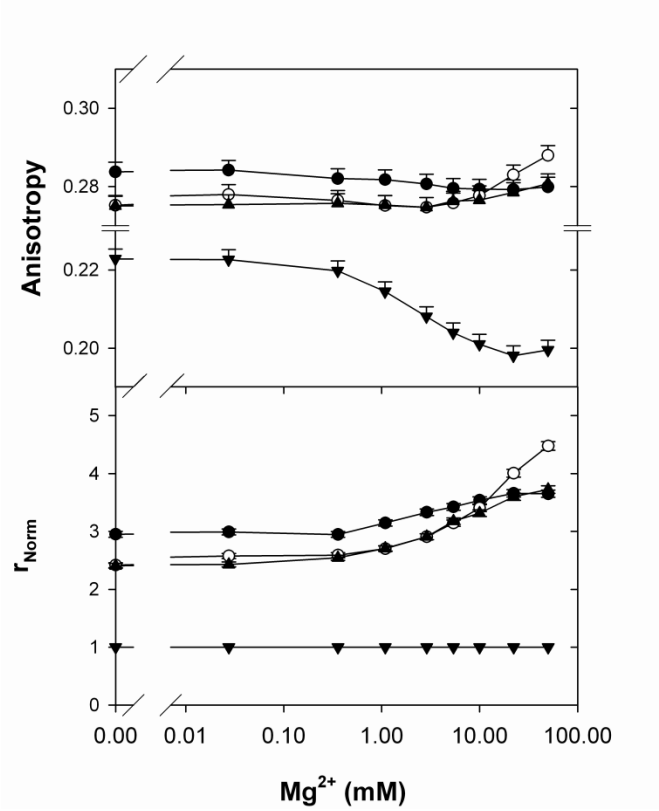

Figure S4

(1) Dehaseth, P. L.; Lohman, T. M.; Record, M. T. *Biochemistry* 1977, *16*, 4783-4790.

(2) Hawkins, M. E. *Nat Protoc* 2007, *2*, 1013-1021.

(3) Hawkins, M. E.; Pfleiderer, W.; Balis, F. M.; Porter, D.; Knutson, J. R. *Anal Biochem* 1997, *244*, 86-95.

(4) Lakowicz, J. R. *Principles of Fluorescence Spectroscopy 3rd edition*; Springer: New York, 2006.

(5) Delatorre, J. G.; Bloomfield, V. A. *Q Rev Biophys* 1981, *14*, 81-139.

(6) Duhamel, J.; Kanyo, J.; DinterGottlieb, G.; Lu, P. *Biochemistry* 1996, *35*, 16687-16697.

(7) Fischer, H.; Polikarpov, I.; Craievich, A. F. *Protein Sci* 2004, *13*, 2825-2828.

(8) Chalikian, T. V.; Breslauer, K. J. *Biopolymers* 1998, *48*, 264-280.

(9) Yguerabi.J; Epstein, H. F.; Stryer, L. *J Mol Biol* 1970, *51*, 573-590.